Numerical Analysis of Thin Skin Depths of 3-D Eddy-Current Problems Using a Combination of Finite Element and Meshless Methods

S. L. Ho, Shiyou Yang, Guangzheng Ni, H. C. Wong, and Yuhuai Wang

***Abstract*—To alleviate the difficulties encountered in the generation of meshes for the finite element method for solving thin skin depth problems involving three-dimensional (3-D) eddy-currents, particularly in cases in which the eddy-current region is only a fraction of the entire domain, a new technique based on the combination of finite element and meshless methods is proposed. The use of numerical approach to uphold the mathematical properties of the combined shape functions in terms of consistency and linear independence is also investigated. It is shown that a very coarse mesh is already sufficient to give accurate numerical results with the proposed algorithm. To validate and demonstrate the advantages of the proposed method, typical numerical results on studies of high-frequency 3-D eddy-current problems are reported.**

***Index Terms*—Eddy-current, finite element method, meshless method, thin skin depth.**

I. Introduction

In the design of high-frequency electromagnetic devices, it is essential to have accurate estimations of the eddy-currents induced in the conducting materials. Although finite element (FE) methods are widely used and recognized as the most powerful numerical technique by academics and engineers alike in solving three-dimensional (3-D) electromagnetic field problems, they are not equally flexible in dealing with all kinds of field problems such as in, for example, large scale thin skin depth 3-D eddy-current problems in which the eddy-current region is only a fraction of the entire domain. For thin skin depth eddy-current problems using 3-D FE methods, one normally has to make a compromise on the need for fine meshes in order to obtain accurate solutions and the heavy demand for computational resources. Thus, a flexible method to add or remove meshes or nodes irrespective of the connectivity of existing meshes or nodes is highly desirable. In this regard, meshless methods are ideal. On the other hand, meshless methods are notoriously difficult when one enforces boundary and interface conditions in solving boundary value problems. To make full use of the advantages of FE and meshless methods, a combined FE and meshless method is proposed for the numerical study of large scale 3-D thin skin depth eddy-current problems to allow one to obtain sufficiently accurate numerical solutions from coarse meshes. In order to separate the meshless and the FE shape functions, bridging scales are added to modify the meshless shape functions to preserve the desirable mathematical properties of the resulting function space in terms of consistency and linear independence. To validate the proposed algorithm, the proposed algorithm is used to solve a prototype high-frequency 3-D eddy-current problem with close-form solutions to facilitate one to assess its numerical performance. Numerical results of eddy-current fields in a cold crucible are used to demonstrate the feasibility of the proposed algorithm for real-word problems.

Manuscript received July 1, 2003.

S. L. Ho is with the Department of Electrical Engineering, the Hong Kong Polytechnic University, Hong Kong (e-mail: eeslho@polyu.edu.hk).

S. Yang is with Department of Electrical Engineering, the Hong Kong Polytechnic University, Hong Kong, on leave from Zhejiang University, Zhejiang, China (e-mail: shiyouyang@yahoo.com).

N.I. Guangzheng and Y. Wang are with the Electrical Engineering College, Zhejiang University, Zhejiang, China (e-mail: nigz@cee.zju.edu.cn; yu_huai@hotmail.com).

H. C. Wong is with the Industrial Center, the Hong Kong Polytechnic University, Hong Kong (e-mail: ichcwong@polyu.edu.hk).

Digital Object Identifier 10.1109/TMAG.2004.824800

II. Mathematical Formulations

A. Moving Least Squares Approximations

The development of the shape function of the proposed meshless method is based on moving least-squares approximation (MLSA). Since the concern of this paper is on the numerical computation of harmonic eddy-current fields, one will restrict one's attention to the interpolation of a complex variable. The local approximation using MLSA for any complex function $\dot{A}(X)(X \in \Omega \subset R^3)$ is

$$\dot{A}_L^h(X) = \sum_{j=0}^{m} p_j(X) a_j(X) = p^T(X)\dot{a}(X) \tag{1}$$

where the unknown parameters $\dot{a}_j(X)$ will vary with X and $p(X)$ is the basis of a complete polynomial of order m [1].

For 3-D problems, $X^T = [x, y, z]$ and a quadratic basis $p^T(X) = [1, x, y, z, xy, yz, zx, x^2, y^2, z^2]$ is used in this paper.

By minimizing some weighted discrete L_2 norm, one can determine the unknown parameters, $\dot{a}(X)$, as

$$\dot{a}(X) = A^{-1}(X)B(X)\,\dot{c} \tag{2}$$

where, $A(x) = \sum_{I=1}^{n} w(X - X_I)p(X_I)p^T(X_I), n$ is the number of nodes in Ω, w is a compactly supported weight function, $[B(X)]_I = w(X - X_I)p(X_I), \dot{c}^T = [\dot{c}_1\ \dot{c}_2\ \cdots\ \dot{c}_n]$, and $\dot{c}_I$ refers to the nodal parameter of $\dot{A}(X)$ at $X = X_I$.

The weight function used in this paper is a cubic spline one [2]. Substituting (2) into (1) yields

$$\dot{A}^h(X) = \sum_{I=1}^{n} \Phi_I^{\text{meshless}}(X)\dot{c}_I \tag{3}$$

where $\Phi_I^{\text{meshless}}(X)$ is the shape function of the meshless method, and is defined as

$$\Phi_I^{\text{meshless}}(X) = p^T A^{-1} B_I \tag{4}$$

It should be pointed out that one of the attractive properties of the MLSA is that the continuity of the shape function is related to the continuity of the weight function [2], hence one could use a linear basis to reproduce higher order continuous approximations by choosing a suitable weight function.

B. Shape Function Modification Considering Consistency

For the proposed method, the meshless method is only used to improve the FE solutions in the thin skin depth of the eddy-current regions. Thus, the approximation of the solution variable in most of the solution domain is expressed in the standard form of FE methods. For the eddy-current regions, the general interpolation formula using both FE and meshless shape functions is

$$\dot{A}(X) = \sum_i \dot{A}_i N_i^{\text{FEM}}(X) + \sum_j \Phi_j^{\text{Meshless}}(X)\dot{c}_j \tag{5}$$

where, $N_i^{\text{FEM}}(X)$ is the FE shape function.

To uphold the mathematical properties of the entire bases regarding consistency and linear independence, the bridge scales as proposed in [3] is used. The basic concept of the bridging scales is based on a hierarchical decomposition of a function $\dot{A}$ which is dependent on some projection operator P to represent, for example, the projection of $\dot{A}$ onto the span of FE shape functions. To decompose the solution variable into two different parts, i.e., the first one that is approximated by meshless shape functions and the second one being represented by the FE shape functions, one employs the property of a projection operator such that multiple projections of the function will leave the function unchanged, i.e., $PP\dot{A} = P\dot{A}$. By using this concept, the total function $\dot{A}$ of (5) can now be reformulated as

$$\dot{A}(X) = \sum_i \dot{A}_i N_i^{\text{FEM}}(X) + \sum_j \Phi_j^{\text{meshless}}(X)\dot{c}_j - \sum_i \sum_j N_i^{\text{FEM}}(X)\Phi_j^{\text{meshless}}(X_i)\dot{c}_j \tag{6}$$

The last term on the right hand side of (6) is called the bridging scale. The reason for including the bridging scale term is to approximate those terms with meshless shape functions to contain only parts of the solution variable which are not included in FE interpolations. Accordingly, the meshless shape function based on the bridging scales becomes

$$\bar{\Phi}_j^{\text{Meshless}}(X) = \Phi_j^{\text{meshless}}(X) - \sum_i N_i^{\text{FEM}}(X)\Phi_j^{\text{meshless}}(X_i) \tag{7}$$

Thus, the general interpolation formula for the proposed combined FE and meshless methods is

$$\dot{A}(X) = \sum_i \dot{A}_i N_i^{\text{FEM}}(X) + \sum_j \bar{\Phi}_j^{\text{Meshless}}(X)\dot{c}_j \tag{8}$$

C. Finite Element Formulation

For simplicity, only the Dirichlet boundary conditions are considered here. Thus, the governing equations for 3-D harmonic eddy-current problems, where the Coulomb gauge is incorporated to guarantee the uniqueness of solutions that use the $\dot{A} - \dot{V}$ method, can be formulated as

$$\nabla \times (\nu \nabla \times \dot{A}) - \nabla(\nu \nabla \cdot \dot{A}) + j\omega\sigma\dot{A} + \sigma\nabla\dot{V} - \dot{J}_s = 0 \tag{9}$$

$$\nabla \cdot (-j\omega\sigma\dot{A} - \sigma\nabla\dot{V}) = 0 \tag{10}$$

where, $\dot{A}, \dot{V}$ are, respectively, the magnetic vector and the electric scalar potentials, ω is the angular frequency of the harmonics, σ is the electric conductivity, ν is the magnetic reluctivity, $\dot{J}_S$ is the source current density.

Using the Galerkin approach with the corresponding weak forms, the discrete form of (9) and (10) become, respectively,

$$\int_\Omega \{\nu\nabla\times \vec{N}_l \cdot(\nabla \times \dot{A}) + \nu\nabla\cdot \vec{N}_l\,(\nabla \cdot \dot{A}) + j\omega\sigma\, \vec{N}_l \cdot\dot{A} + \sigma\, \vec{N}_l \cdot\nabla\dot{V} - \vec{N}_l \cdot\dot{J}_S\}\, dV = 0 \tag{11}$$

$$\int_\Omega \nabla\, \vec{N}_l \cdot(j\omega\dot{A} + \sigma\nabla\dot{V})\, dv = 0 \tag{12}$$

where, $\vec{N}_l$ is the weighting function.

To transform (11) and (12) into symmetric forms, a transformation

$$\dot{V} = j\omega\dot{V}', \tag{13}$$

is used. (11), (12) can be reformulated by using matrix equations as shown in (14) at the bottom of the page.

Substituting (8) into (14) and selecting $\vec{N}_l = N_i^{\text{FEM}}$ or $\vec{N}_l = \bar{\Phi}_j^{\text{Meshless}}$, one will obtain the discrete mathematical model of the proposed method.

III. Numerical Examples

A. Validation

To validate the feasibility of the proposed algorithm for solving thin skin depth harmonic eddy-current problems and to compare the numerical results with their corresponding analytical solutions, the electromagnetic fields around a circular conductor carrying a 20-kHz harmonic current flowing in the z direction as shown in Fig. 1 is investigated. The radius of the circular conductor is 2 mm. By setting a cylindrical surface, S_1, which is co-centered with the conductor and is sufficiently far from the conductor surface, S_3, such that the field on S_1

$$\begin{bmatrix} \int_\Omega [\nu\nabla\times \vec{N}_l \cdot\nabla\times(\,) + \nu\nabla\cdot \vec{N}_l\,\nabla\cdot(\,) + j\omega\sigma\, \vec{N}_l \cdot(\,)]\, dv & \int_\Omega j\omega\sigma\, \vec{N}_l \cdot\nabla(\,)\, dv \\ \int_\Omega j\omega\sigma\nabla\, \vec{N}_l \cdot(\,)\, dv & \int_\Omega j\omega\sigma\, \vec{N}_l \cdot\nabla(\,)\, dv \end{bmatrix} \cdot \begin{Bmatrix} \dot{A} \\ \dot{V}' \end{Bmatrix} = \begin{Bmatrix} \int_\Omega \vec{N}_l \cdot\dot{J}_s dv \\ 0 \end{Bmatrix} \tag{14}$$

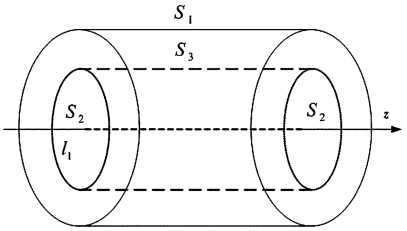

Fig. 1. Circular conductor carrying a 20-kHz harmonic current flowing in the z coordinate direction.

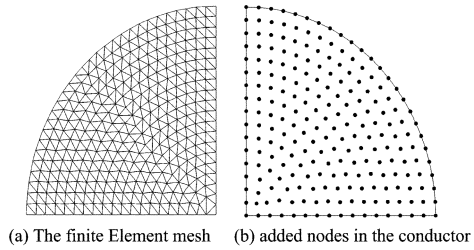

Fig. 2. FE mesh and the node arrangement of the proposed method on Surface S_2. (a) The FE meshes and (b) scaled view of the conductor region showing the additional meshless nodes.

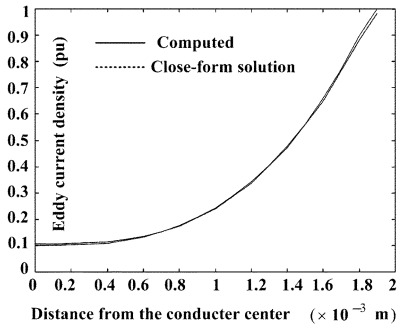

Fig. 3. Comparison of the computed and close-form eddy-currents in the conductor.

can be approximated as zero, the boundary conditions for this pseudo-3-D eddy-current problem are

$$\dot{\mathrm{A}}_{\mathrm{x}}|_{\mathrm{S}_1} = \dot{\mathrm{A}}_{\mathrm{y}}|_{\mathrm{S}_1} = \dot{\mathrm{A}}_{\mathrm{z}}|_{\mathrm{S}_1} = 0$$
$$\dot{V}'|_{l_1} = 0, \quad \vec{n} \times \dot{\vec{A}}|_{S_2} = 0, \quad \frac{\partial A_z}{\partial n}|_{S_2} = 0 \qquad (15)$$

where, $\vec{n}$ is the normal direction of surface S_2.

In the numerical implementation, the entire domain is divided into two different parts, i.e., the conductor part and the residual of the solution domain that contains the surrounding free space. In the conductor, both FE and meshless shape functions contribute to the interpolation. In the latter region, only FE has influences. For the proposed method to work, the solution domain is firstly discretized into a coarse FE mesh in which the mesh size is about the skin depth of the harmonic current. Some nodes are then added into the thin skin depth eddy-current region (the conductor) as shown in Fig. 2 such that the maximum distance between neighbor nodes in the conductor is less than one-fourth of the skin depth. Comparison of the accuracy of the computed results using the proposed method with the close-form solutions is given in Fig. 3. The distribution of the eddy-current in the conductor is shown in Fig. 4. The distribution of the magnetic flux density along the radial direction is shown in Fig. 5. To

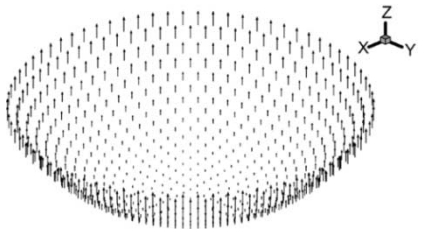

Fig. 4. Distribution of the eddy-current density in the conductor.

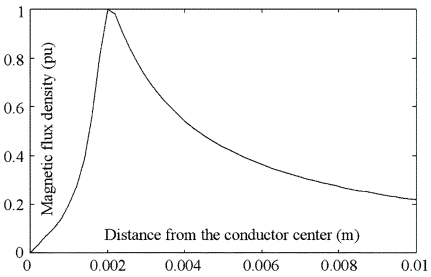

Fig. 5. Distribution of the magnetic flux density along the radial direction.

TABLE I
PERFORMANCE COMPARISON OF THE PROPOSED AND PURE FE METHODS HAVING THE SAME LEVEL OF SOLUTION ACCURACIES

	DoFs	CPU time (Minutes)
Pure FE method	13480	5.2
The proposed method	6428	4.9

compare the performances of the proposed with the purely FE methods, this problem is repeatedly solved using a purely FE method by successively increasing the mesh density, especially in the conductor to make the mesh size less than one third of the skin depth, until the same accuracy as that of the proposed method is obtained. The corresponding performance comparison results are given in Table I. From these numerical results, it is very clear that: 1) the results of the computed eddy-current distribution of the proposed method and those obtained from the close-form expression are nearly the same, and they are indeed indistinguishable in the figure; 2) besides producing nearly exact solutions of the eddy-current fields in the conductor where both FE mesh and meshless nodes are used, the proposed algorithm also produces very accurate far end magnetic flux density results even if very coarse FE meshes are used; 3) for the same level of numerical accuracies, both the degree of freedom (DoF) and the solution time of the proposed algorithm are less than those of the purely FE method.

B. Application

The high-frequency eddy-current fields in a cold crucible are solved using the proposed algorithm to demonstrate its feasibility in solving practical problems. A cold crucible is a high-frequency induction melting furnace with conductive walls segmented by longitudinal slits. Each electrically isolated segment is internally or externally cooled by water. These kinds of crucibles have the rapid Joule heating capacity of conductive materials that do not make contact with the walls due to the strong pinching force arising from interactions of the imposed electromagnetic field and the induced electric current in the molten metal [4]–[6]. The crucibles have excellent performances when they are used to re-melt high melting-point or chemically active

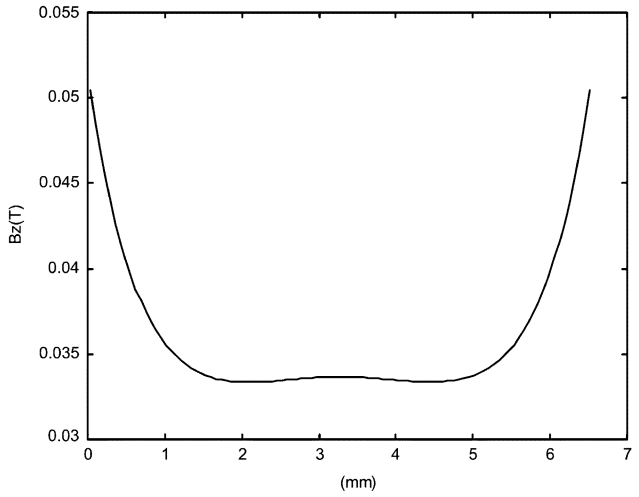

Fig. 6. Distribution of the computed magnetic flux density in one segmental region on the predefined path along the circumferential direction under the influence of a 20-kHz harmonic current.

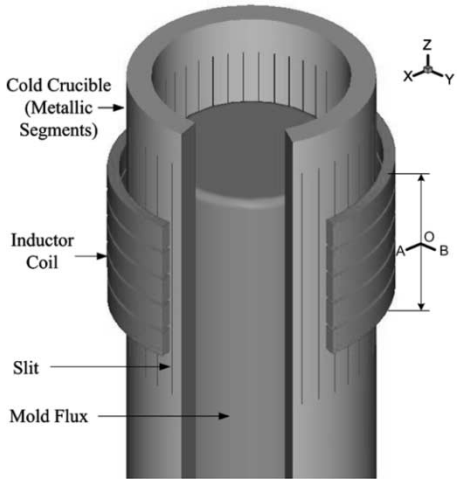

Fig. 7. Schematic diagram of a cold crucible.

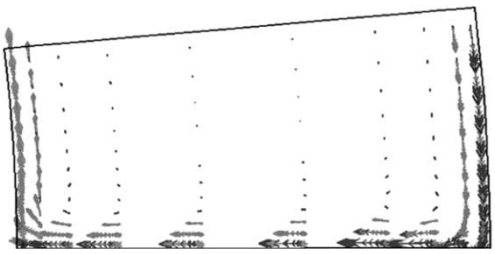

Fig. 8. Eddy-current distribution in half of one segment in plane A-O-B.

materials if there is no contamination or no chemical reactions between the molten materials and crucible materials.

To realize the optimal design of a cold crucible, it is essential for one to have a clear understanding of the 3-D eddy-current fields. However, it is very hard, if not impossible, to conduct these studies experimentally. Thus numerical simulation is the most appropriate approach. Consequently, a closed slit prototype crucible [5] is selected as the numerical example. Due to symmetry, only one-fourth of the regions are modeled. In the figures hereafter, both the sample points and the specified path are on the surface of the molten metal. Fig. 6 depicts the computed magnetic flux density distribution in one segmental region on a predefined path when a 20-kHz harmonic current is applied to the coils. The path is defined as a circumferential circle, which lies on the plane A-O-B, along the circumferential direction. As shown in Fig. 7, the plane A-O-B passes through the center of the coil in the z direction. The eddy-current distribution in half of one segment in plane A-O-B is shown in Fig. 8. The distribution of the computed magnetic flux density of the slits along the z coordinate (axial) direction is shown in Fig. 9. Clearly, these numerical results positively confirm the feasibility of the proposed algorithm in solving practical large scale 3-D thin skin depth eddy-current problems.

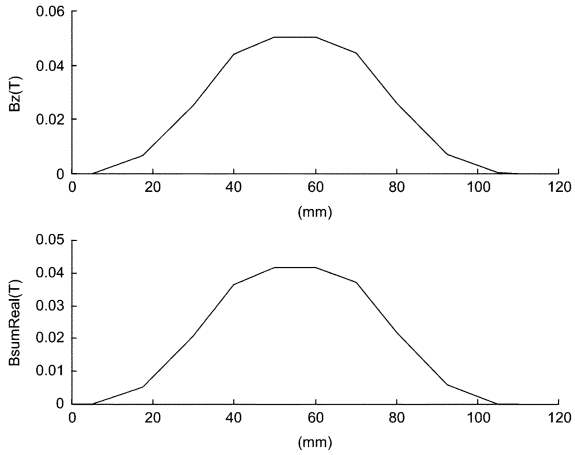

Fig. 9. Distribution of the computed magnetic flux density in the slit along the z coordinate direction with a 20-kHz harmonic current.

IV. Conclusion

A combined FE and meshless method for studying thin skin depth of eddy-current problems is proposed. Compared with other approaches, the proposed method allows one to have the flexibility to add nodes in some specific regions without the need to consider their connectivity in the numerical implementation, thereby allowing one to have a minimal DoF to obtain sufficiently accurate numerical results. The accuracy and feasibility of the proposed model are validated by studying the numerical results of two different high-frequency eddy-current problems as reported in this paper.

References

[1] T. Belytschko, Y. Y. Lu, and L. Gu, "Element-free Galerkin methods," *Int. J. Numer. Meth. Eng.*, vol. 37, pp. 229–254, 1994.

[2] J. Dolbow and T. Belytschko, "An introduction to programming the meshless element free Galerkin method," *Arch. Computational Meth. Eng.*, vol. 5, no. 3, pp. 207–241, 1998.

[3] G. J. Wagner and W. K. Liu, "Hierarchical enrichment for bridging scales and mesh-free boundary conditions," *Int. J. Numer. Meth. Eng.*, vol. 50, pp. 507–524, 2001.

[4] H. Makino, M. Kuwabara, and S. Asai, "Process analysis of noncontact continuous casting of materials using cold crucible," *ISIJ Int.*, vol. 36, pp. 380–387, 1996.

[5] N. Yoshida, S. Furuhashi, and T. Tanka, "Newly designed stiff EMC mold with imposition of super-high frequency electromagnetic field," in *Proc. 3rd Int. Symp. Electromagnetic Processing of Materials*, 2000, pp. 388–391.

[6] M. Feliachi, D. Benzerga, F. Z. Louai, and G. Develey, "On the 2D or 3D coupled analytical and finite element analysis of eddy-current and thermal problems in Plasma devices," *IEEE Trans. Magn.*, vol. 32, pp. 1613–1616, May 1996.